A NOVEL DESIGN OF A LOCOMOTION SYSTEM FOR ACTIVE CAPSULE ENDOSCOPY

Ahmad M. Alshorman*, Omar A. Ababneh, Anas I. Abushaker,
Emran M. Tamimi, Osama Z. Bani-yassin
Mechanical Engineering Department
Jordan University of Science and Technology
Irbid, Jordan 22110
amalshorman6@just.edu.jo

2021 7th International Conference on Mechatronics and Robotics Engineering (ICMRE) | 978-1-6654-1489-0/21/$31.00 ©2021 IEEE | DOI: 10.1109/ICMRE51691.2021.9384823

***Abstract*—The active endoscopy system has a locomotion system that allows the endoscopist to control the capsule's motion in the GI tract. The endoscopist can move, or stop the capsule at any targeted locations, which provides a better and more reliable diagnosis. We propose a novel design of a capsule's locomotor with shape memory alloy (SMA) actuators. The hinge mechanism to translates the linear movement of the SMA into a translational motion to the capsule's links. The proposed design has the added advantage of steering the capsule's camera system by activating one or more SMA wires. To the best of our knowledge, this is the first proposed active capsule that has a steering mechanism that controls the camera view angle at the top of the capsule. This camera's steering mechanism leads to a wider angle range for the system without adding to the capsule's weight and size. Also, this will help to better capture pathological areas without increasing power consumption. The proposed capsule prototype is manufactured using 3D printing technology and powered by a battery installed in the capsule.**

***Index Terms*—Capsule Endoscopy, Locomotion, Active Capsule Endoscopy, Biorobotics.**

I. Introduction

Endoscopy is a non-surgical process in which the digestive tract is photographed for examination and therapeutic purposes. Endoscopy also Makes an initial diagnosis of Inflammatory bowel disease (IBD), distinguishes Crohn's disease, and ulcerative colitis [12]. Endoscopy procedures were revolutionized by introducing a miniature robot equipped with a camera and sometimes a means of locomotion or biopsy, which will travel through the whole gastrointestinal (GI) tract after swallowing the capsule [5]. Capsule endoscopy became a replacement option in many cases to conventional endoscopy. It has the advantage of being a painless process, and it helps to reach the whole gastrointestinal (GI) tract like the small intestine, which cannot be reached by traditional endoscopy [5]. Also, the endoscopists will need less skill because of the simple procedure, thus reducing the training time.

Capsule endoscopy is classified as passive or active capsule endoscopy. Passive capsule endoscopy is a capsule that relies on GI peristalsis to move, as the capsule's movement and the camera can not be controlled. All commercially available capsules are passive capsules, proving their efficiency and success in diagnosing and identifying many GI tract diseases.

Address all correspondence to this author.

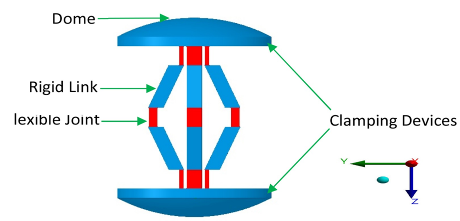

Fig. 1: The Components Of The Capsule

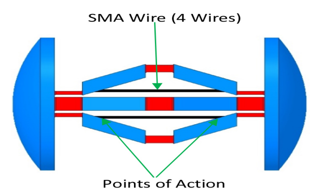

Fig. 2: SMA Wires' Placement

Active capsule endoscopy is a capsule that does not rely entirely on peristalsis; these capsules can stop, change their direction and speed. These capsules allow the endoscopist to control the capsule and have better control over the operation; this improves the detection and diagnosis of pathological areas, thus increasing the reliability [11], [13]. In the active capsules, there are three more sub-systems to implement: the actuator, the attachment mechanism, and the nature of the locomotion mechanism [2], [3]. Different alternatives within those sub-systems will be briefly discussed. Also, different adoptions of these alternatives usually are what distinguish between different capsule propositions within the literature.

Locomotion is a way to describe how the mechanism of the robot's motion. There is a wide variety of locomotion techniques, and mechanisms [1], [3], [4]. In the proposed novel design, the inchworm locomotion mechanism is used. The inchworm movement is achieved by a sequence of expansions and contractions of the capsule; these sequences are produced due to the process of turning on and off the shape memory alloy wires and the hinge mechanism. By restricting the backward movement using an attachment mechanism, a forward movement is achieved. Hence, the attachment mechanism repeatedly provides friction without damaging the

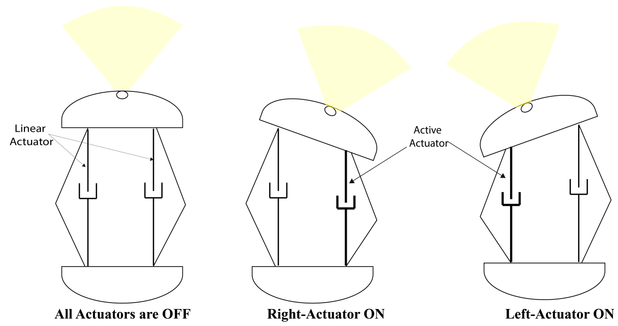

Fig. 3: Camera's Steering Mechanism

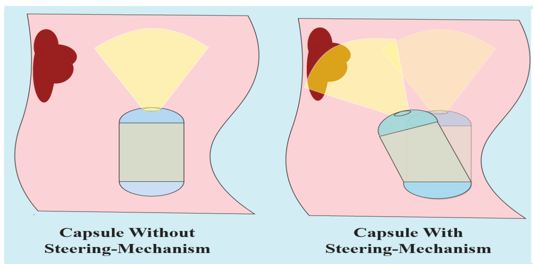

Fig. 4: Steering Mechanism To Increase The View Angle

gastrointestinal (GI) tract. The animal kingdom is a huge inspiration to engineers with numerous mechanisms [7], [14]. Some researchers implemented the spacer [8] and others implemented micro-patterned adhesives [6], while others implemented micro-hooks [10]. Bearing in mind the proposed mechanism's limited space and high-power consumption (due to the SMA wire), the micro-hooks attachment mechanism is preferable, even though it lacks a stopping mechanism and the ability to move backward [9], [15].

Micro-actuators convert the electric energy in the battery to the mechanical movement that excites the capsule. Due to size constraints, the actuation mechanism in capsule endoscopy is limited to a few options, namely Piezoelectric material, DC motor, SMA, and Ionic polymer-metal composites (IPMC). Due to the suggested mechanism's nature, the beneficial micro-actuators would be SMA and Piezoelectric, but SMA was favored for the additional developed force and the significant displacement. The extra developed force has the benefit of minimizing the risk of retention. Table (1) provides a general comparison between the main micro-actuators used in literature.

Due to biological constraints, some parameters should be within a specific range, such as the temperature and the

TABLE I: A General Comparison Between Micro-Actuators

	Piezo-Electric	**DC Motor**	**SMA**	**IPMC**
Voltage	High	Low	Low	Low
Controllability	Good	Good	Not easy	Not Easy
Displacement	Low	Rotation	Linear	Bends
Force	Low	High	High	High
Frequency	High	High	Low	
Size/Weight	Good	Large	Good	Good

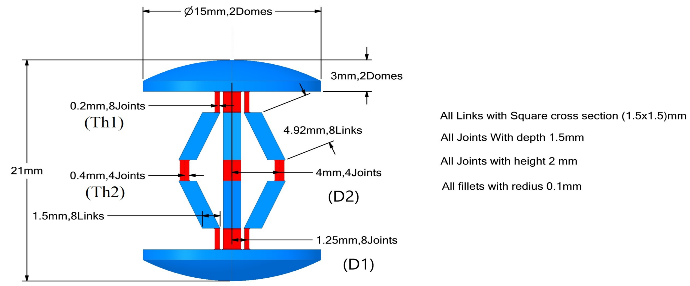

Fig. 5: The Capsule's Dimensions

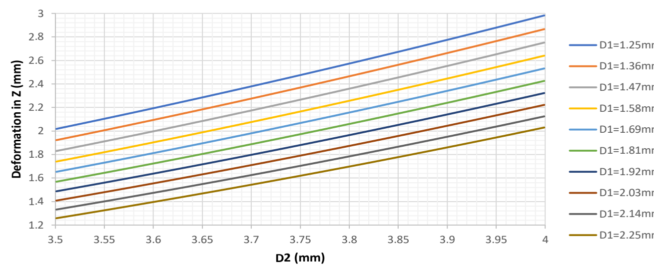

Fig. 6: Deformation In Z Direction Against D1 And D2 (mm).

capsule's size. The temperature of the SMA wire should not increase the limit that may damage the tissue, and the capsule could be packaged in a way to reserve this constraint.

The proposed mechanism consists of four bendable links (the mechanism structure), and two domes that hold the necessary components: the power module, the camera, and the control unit. An SMA wire will hold the opposite sides of each link. When the SMA wire contracts, the capsule will contract, and in the presence of the micro-hooks, the capsule will move forward. The proposed novel design is particularly advantageous at changing the camera's angle without an extra steering mechanism; this is achieved by actuating several of the four legs, which will steer the dome in the desired direction. Also, upon contraction, the capsule's size is minimal, making swallowing the capsule easier.

The four legs used in the capsule are considered compliance mechanisms with flexure hinges. Flexure hinges are used in a compliant mechanism to transform load, motion, and energy by deformation. Flexure hinges are divided into two groups, (a) lumped compliance and (b) distributed compliance. Moreover, the one used in this mechanism is lumped compliance.

II. MATERIALS AND METHODS

In the design of the compliant mechanism, a systemic method was followed. First, the topology synthesis was done, making a feasible functional design of the whole capsule, starting from input/output (force/motion) specifications. The initial design was conducted using reliable 3D-CAD design software (Solidworks software). The dimensions were roughly chosen within the capsule endoscopy's biological constraints, generally, to be optimized later. The structural analysis is conducted using the finite element method (FEM)-ANSYS Multiphysics software.

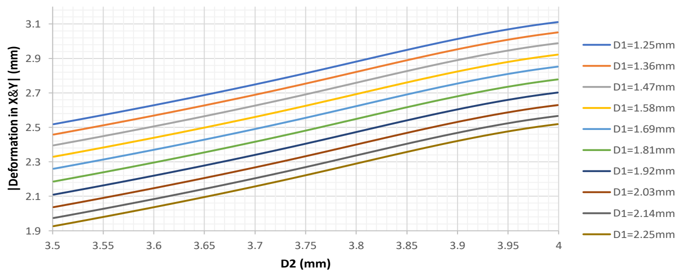

Fig. 7: Deformation In X And Y Directions Against D1 And D2 (mm).

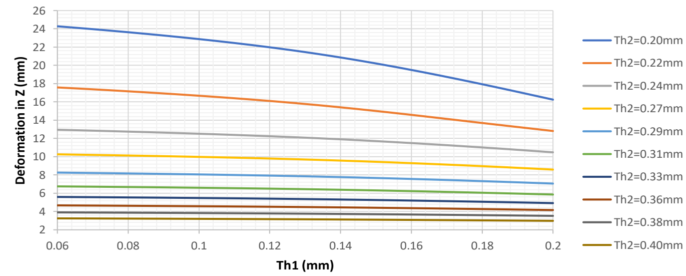

Fig. 9: Deformation In Z Direction Against Th1 And Th2 (mm).

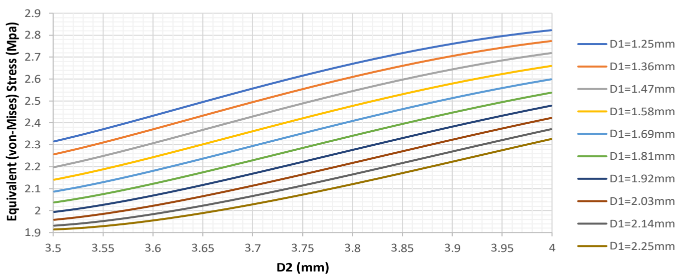

Fig. 8: Equivalent (Von-Mises) Stress Against D1 And D2 (MPa).

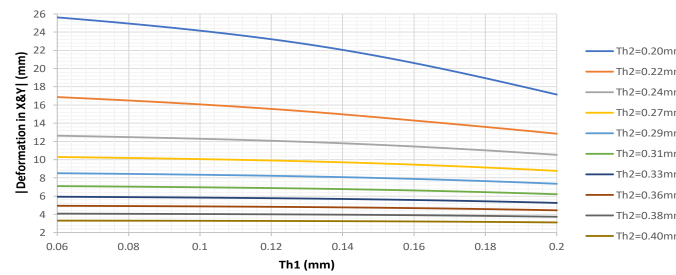

Fig. 10: Deformation in X,Y Directions Against Th1 and Th2.

An optimization technique was conducted to get the capsule's optimal design, materials, and maximize the capsule's speed and widen the camera's angle. The flexure hinges in the middle of the capsule have the highest effect on stress and deformation. Thus, the optimization was conducted to design the flexible joint and its thickness to get the highest deformation (locomotion-speed) with a reliable factor of safety.

A. Proposed mechanism

The mechanism proposed consists of eight rigid links, twelve flexible joints, and two domes. The domes hold the necessary components like the power module, the camera, and the control unit. Clamping devices are in the side area of the domes, and they will provide friction during locomotion, as shown in fig. 1. Four SMA wires are placed on the links between the upper and lower dome, as shown in fig. 2 when the SMA wires are actuated the capsule contracts. This allows for the possibility of steering the camera with the same mechanism used for locomotion. This is done by actuating several links causing the dome and the camera to tilt, as shown in fig.3. At certain spots of the small intestine, where the pathology is located, it would be helpful to hold the capsule in place to further inspect the lesion, to take views with extra angles, to diagnose with tissue sampling, or to intervene with drug delivery, bleeder clipping or with the application of any other maneuver fig.4. The capsule's view angle can be improved using the proposed steering mechanism. The final capsule dimensions are shown in fig. 5. The overall length of the capsule is $21mm$ which is within biological constraints (i.e.$30mm$), and the diameter of the two domes is $15mm$ which is within biological constraints (i.e. $15mm$).

The effect of changing dimensions D1 and D2 (see fig.5) were studied to show the maximum deformation in the X and Y directions under the full load. Due to symmetry, the deformation in X and Y is the same. The joints must not peak out of the capsule, which happens at the joint's deformation of $(3mm)$, as shown in fig.7.

B. 3D Printing materials

The material selection is based on biocompatibility, mechanical properties, and flexibility. Furthermore, each material's printing temperature must be taken into consideration since the design involves two materials that will be printed on top of each other. Table (II) shows the different types of materials, and table (III) shows the properties of these materials.

C. Finite Element Analysis and simulation

The finite element analysis (FEA) was conducted to optimize three parameters:

- The Equivalent (Von-Mises) Stress, which must not exceed the yield stress of the weakest material (i.e., TPU).
- The deformation in the X and Y directions must not exceed $3mm$ (that is, the distance between the outer surface of the joint and the boundary of the capsule) so the joints do not peak out of the capsule's boundary.
- Maximizing the deformation in the Z direction correlates to the capsule's speed and locomotion.

With these parameters in mind, joints size and shape are the determining factors of the optimization because:

- They have the lowest yield stress of the entire mechanism and are subject to the largest stress.

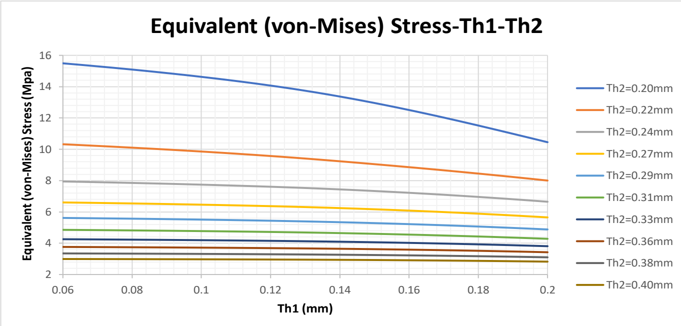

Fig. 11: Equivalent (Von-Mises) Stress Against Th1 and Th2.

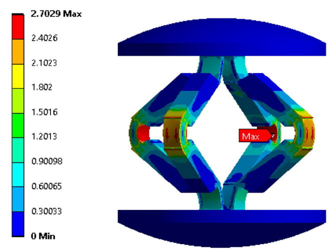

Fig. 12: Stress Results After Applying the 0.67N Force

- When in contraction, the joints are what increase the X and Y directions deformation.
- The deformation in the Z direction is correlated to the deformation of the joints.

Several different shapes were studied and optimized, and the rectangular shape was preferred due to the ease of manufacturability and its effectiveness. Two factors were optimized in the joint:

- The distance from the flexible joint to the capsule's center (D1 and D2, see fig.5).
- The thickness of the flexible (Flexure hinge) joints (Th1 and Th2, see fig.5).

The resulting steering angle was also studied. The angle proportionally increases with force with an of 42 degrees.

III. Kienmatic and Dynamic Model

Compliant mechanisms perform their motion through monolithic flexible members that deform under the actuation of external load. Hence, the flexure hinge (FH) is the essential part of compliant mechanisms which is a thin region that provides limited relative rotation between two adjacent rigid links under actuation of external loading mainly through the bending process.

Therefore, the compliant mechanism obtains its functionality by transferring an input form of energy (mechanical, electric, thermal, magnetic, etc.) into output motion by the way of elastic deformation of the flexure hinge. The dynamic modeling of the compliant mechanism is mainly pertained to obtain a specific response under dynamical loading. This modeling and corresponding response depend on the compliance or conversely the stiffness of flexure hinges that form the device alongside the mechanism structure and load definition.

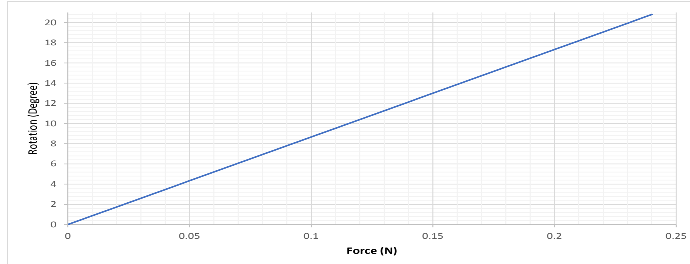

Fig. 13: Steering Angle (Rotation) Against the Applied Force.

TABLE II: Different Combinations of 3D Printing Materials

Rigid Components	Complaint Joints
PLA	PLA
PLA	TPU
ABS	ABS
ABS	TPU

Based on Pseudo-Rigid-Body-Model (PRBM) , the simple model considers the two-dimensional FH as a torsional spring that is compliant only about one axis and much stiff about all other axes; in other words, it performs pure rotation about one degree of freedom (DOF). Where the stiffness of the hinge flexure is given by:

$$K = \frac{E.I_H}{L} \tag{1}$$

Where E is modulus of elasticity of the flexure hinge, I_H is the moment of inertia of FH, and L is the length of flexure hinge.

For the sake of simplicity, we introduce a simple model for each link of the capsule by neglecting the translational motions in X and Y directions of the flexible part. So, only rotational motion of the flexible link will be considered. As a result, the rotational motion of Newton's second law with simple hinge stiffness that given by eq.1 is given by:

$$\sum M = I\ddot{\theta} \tag{2}$$

where I is the moment of inertia, $\ddot{\theta}$ is the rotational acceleration,M is the applied torque on the FH. The torque has two components. The first components is the torque produced by the force of the SMA actuator on the rigid links (τ_{SMA}). The second components is the elastic torsional torque of the flexure hinge (τ_{FH}).

$$\tau_{FH} = K.\theta \tag{3}$$

and

$$\tau_{SMA} = F_{SMA}.d \tag{4}$$

Where d is the distance between the SMA wire and the center of the FH. and the F_{SMA} is the applied force of the SMA actuator. The SMA wire strain rate $\dot{\epsilon}$ and flexible joint angular velocity $\dot{\theta}$ are related kinematically as

$$\dot{\epsilon} = \frac{L.\dot{\theta}}{L_w} \tag{5}$$

Where L is the rigid link length, L_w the undeformed length of the SMA wire.

TABLE III: Mechanical Properties of 3D Printing Materials

Rigid- Components	E(MPa)	N	$\rho(Kg/m^3)$
ABS	**40**	0.35	1050
PLA	**65**	0.36	1240
TPU	**4**	0.48	1190

IV. RESULTS AND DISCUSSION

In this study, we optimize our design to get higher joints deflection with lowest stress possible. Though, In fig.6 D1 and D2 were studied against the Z direction's deformation under the full load of $0.7N$ ($0.175N$ per link). The Z-axis deformation in the Z direction will increase, but the stress and the deformation in the X and Y directions will also increase, and both of which should be under a certain limit.

The same dimensions were studied against the maximum equivalent von-mises stress under the full load; the stress must be less than the capsule's yield stress ($4MPa$), as shown in fig.8. The deformation was studied under the full load, thinner joints will increase the deformation, but it will also increase the joint's stress, as shown in fig.9 and fig.10.

Due to the limitation of $3mm$ on the deformation in the X and Y directions, the thicknesses Th1 and Th2 are restricted to $0.2mm$ and $0.4mm$, respectively, as shown in fig.10.

The degree of rotation is maximum at the full force $0.24N$ (on each link), almost at 21^o, which increases the field of view of the camera by 42^o, and the relationship between the force applied and the rotation is linear as shown in fig.(13).

The stresses at the chosen thicknesses are below the yield stress of $4MPa$, as shown in fig.11. The dimensions chosen for D1 and D2 were $1.25mm$ and $4.00mm$, respectively. Although the links peak out of the capsule at these dimensions, a lower force ($0.67N$) will be applied to prevent it, which will also help reduce the power consumption. The FEA stress analysis result at these values under the full load ($0.67N$ or $0.1675N$ on each link) is shown in fig. 12. The maximum Von-Mises stress was on the mid joints at $2.7MPa$, giving a safety factor of 1.48. And the deformation in the Z direction at these dimensions is $2.85mm$.

In summary, optimization of four factors (i.e., D1, D2, Th1, and Th2) was done against three factors or limitations. The first factor was that the links should not peak out of the capsule (this is the deformation in the X and Y directions). The second one is that the maximum stress should not exceed the yield stress, finally maximizing the Z direction's deformation. The chosen dimensions at the load $0.1675N$ per link were D1 = $1.25mm$, D2 = $4.00mm$, Th1 = $0.20mm$, and Th2 = $0.40mm$. The analysis results at those values are, the maximum stress was $2.7MPa$ compared to $4MPa$ yield stress (which gives a factor of safety of 1.48) and the maximum deformation in the Z direction was $2.85mm$.

V. CONCLUSION

Capsule endoscopy is an important device that overcomes traditional endoscopy difficulties, especially active capsule endoscopy, which allows the doctor to get a clear perspective on the GI tract's infected area. In this research, a new design of active capsule endoscopy was proposed; this design allowed the capsule's locomotion and steering in a single mechanism. The proposed mechanism increases the view of the camera by 42^o and contracts by $2.85\ mm$.

ACKNOWLEDGMENT

This work is supported by King Abdullah II Fund For Development (KAFD) under Project Number 2020/9.

REFERENCES

[1] Ahmad Alshorman. Design and control of microgripper system. Master's thesis, Jordan University Of Science And Technology, 2011.

[2] Ahmad Alshorman. *Dynamics and control of particle based, chain mechanism*. PhD thesis, Southern Methodist University, 2015.

[3] Ahmad Alshorman and Yildirim Hurmuzlu. Kinematic locomotion modes of particle-based linear chain mechanisms. *Journal of Dynamic Systems, Measurement, and Control*, 140(2), 2018.

[4] Paolo Dario and CA Mosse. Review of locomotion techniques for robotic colonoscopy. In *2003 IEEE International Conference on Robotics and Automation (Cat. No. 03CH37422)*, volume 1, pages 1086–1091. IEEE, 2003.

[5] Hiroki Endo, Yasuyuki Kondo, Masahiko Inamori, Tomohiko R Ohya, Tatsuro Yanagawa, Masako Asayama, Kantaro Hisatomi, Takuma Teratani, Masato Yoneda, Atsushi Nakajima, et al. Ingesting 500 ml of polyethylene glycol solution during capsule endoscopy improves the image quality and completion rate to the cecum. *Digestive diseases and sciences*, 53(12):3201–3205, 2008.

[6] Paul Glass, Eugene Cheung, and Metin Sitti. A legged anchoring mechanism for capsule endoscopes using micropatterned adhesives. *IEEE Transactions on Biomedical Engineering*, 55(12):2759–2767, 2008.

[7] Stanislav N Gorb. Biological attachment devices: exploring nature's diversity for biomimetics. *Philosophical Transactions of the Royal Society A: Mathematical, Physical and Engineering Sciences*, 366(1870):1557–1574, 2008.

[8] Shu He, Guo-Zheng Yan, Quan Ke, Zhi-Wu Wang, and Wen-Wen Chen. A wirelessly powered expanding-extending robotic capsule endoscope for human intestine. *International Journal of Precision Engineering and Manufacturing*, 16(6):1075–1084, 2015.

[9] Qais Khasawneh, Mohammad A Jaradat, and Ahmad Alshorman. Enhanced design of microgripper using double actuators of shape memory alloy wires. In *ASME 2014 Dynamic Systems and Control Conference*. American Society of Mechanical Engineers Digital Collection, 2014.

[10] Byungkyu Kim, Sunghak Lee, Jong Heong Park, and Jong-Oh Park. Design and fabrication of a locomotive mechanism for capsule-type endoscopes using shape memory alloys (smas). *IEEE/ASME transactions on mechatronics*, 10(1):77–86, 2005.

[11] Anastasios Koulaouzidis, Dimitris K Iakovidis, Alexandros Karargyris, and Emanuele Rondonotti. Wireless endoscopy in 2020: Will it still be a capsule? *World journal of gastroenterology: WJG*, 21(17):5119, 2015.

[12] Jonathan A Leighton, Bo Shen, Todd H Baron, Douglas G Adler, Raquel Davila, James V Egan, Douglas O Faigel, Seng-Ian Gan, William K Hirota, David Lichtenstein, et al. Asge guideline: endoscopy in the diagnosis and treatment of inflammatory bowel disease. *Gastrointestinal endoscopy*, 63(4):558–565, 2006.

[13] Lin Lin, Mahdi Rasouli, Andy Prima Kencana, Su Lim Tan, Kai Juan Wong, Khek Yu Ho, and Soo Jay Phee. Capsule endoscopy—a mechatronics perspective. *Frontiers of Mechanical Engineering*, 6(1):33–39, 2011.

[14] Werner Nachtigall. *Biological mechanisms of attachment: The comparative morphology and bioengineering of organs for linkage, suction, and adhesion*. Springer Science & Business Media, 2013.

[15] Yosri Taha Sanaani, Ahmad Alshorman, and Khaled Alshurman. A novel design of flexure based, shape memory alloy actuated microgripper. In *ASME 2017 International Mechanical Engineering Congress and Exposition*. American Society of Mechanical Engineers Digital Collection, 2017.